

Supporting Information

Optical Dark Field and Electron Energy Loss Imaging and Spectroscopy of Symmetry-Forbidden Modes in Loaded Nanogap Antennas

T. Brintlinger,¹ A. Herzing,² J. P. Long,³ I. Vurgaftman,⁴ R. Stroud,¹ and B. S. Simpkins^{3,*}

¹Materials Division, Naval Research Laboratory, 4555 Overlook Ave. SW, Washington D.C. 20375, United States

²Materials Measurement Laboratory, National Institute of Standards and Technology, Gaithersburg, MD, United States

³Chemistry Division, Naval Research Laboratory, 4555 Overlook Ave. SW, Washington D.C. 20375, United States

⁴Optical Sciences Division, Naval Research Laboratory, 4555 Overlook Ave. SW, Washington D.C. 20375, United States

*Corresponding author, blake.simpkins@nrl.navy.mil

Resonant modes of single gold rod

Single Au rods were prepared using templated electrochemical deposition, released, cleaned, and drop-cast onto an ITO/glass substrate. These structures are a building block of the more complex hybrid system and provide a baseline for expected resonant behavior. Optical dark field scattering of such structures exhibit two degenerate transverse modes (in-plane and out-of-plane) which split due to substrate interactions and a longitudinal mode. These are all shown in Figure S1.

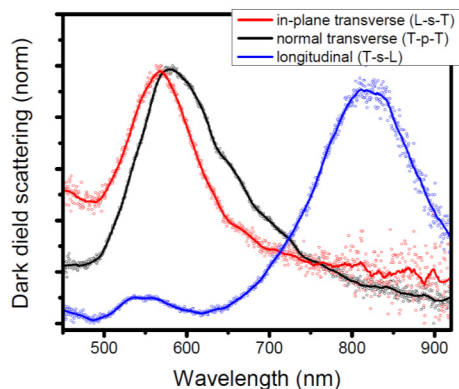


Figure S1. Scattering spectra acquired for a single Au rod on an ITO/glass substrate. Out-of-plane transverse mode (black) exhibits red-shift relative to in-plane transverse mode (red) due to substrate-induced degeneracy lifting. Longitudinal band (blue) is located ~ 825 nm.

Longitudinal mode dispersion with length

Due to the ~10-15% variation in growth rate for rods housed in different pores, we produced nanogap antennas whose arms varied in length from ~110 to 170 nm. In Figure S2, we plot the spectral position of the longitudinal mode as a function of arm length. In cases where the two arms are not exactly the same length, the longer arm length was used since it is expected to scatter more strongly and dominate the scattering spectrum. As seen, the longitudinal mode disperses red with increased length (slope ~ 0.55). This is expected and qualitatively consistent with simulation results, however, our simulation results for ideal structures (right cylinders with perfectly flat interfaces between materials) disperse at a faster rate (slope ~ 2). A weakened dispersion with length in air-gap nanogap antennas has been reported¹ and was attributed, as we do here, to non-idealities present in the experimentally realized structures.

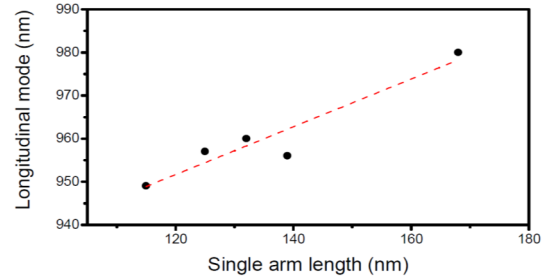


Figure S2. Dispersion of longitudinal mode position with nanogap antenna arm length. The resonance moves red as arm length increases, albeit less rapidly than expected from single-rods or simulations, possibly because this mode is also effected by gap size, end- and interface-morphologies, and non-idealities in the fabricated structures.

Full set of optical dark field scattering data

Allowing for 2 principle orientations for incident light direction, excitation orientation, and detection polarization, yields eight possible experimental geometries. A full set of scattering spectra for a nanogap antenna are given in Figure S3. Of note is the L-p-L geometry (red curve) which reveals all three modes in a single measurement. This geometry excites the conventional and gap-localized transverse modes since it employs an out-of-plane excitation but it also excites the longitudinal mode, presumably due to the small longitudinal component to the excitation field. The L collection polarization acquires scattering from all of these modes while T collection (orange curve) is limited to only the transverse modes.

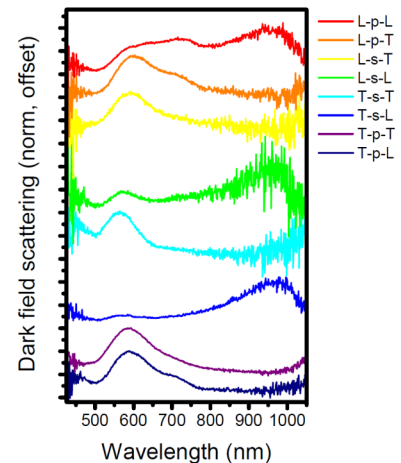


Figure S3. Full set of scattering spectra from a single nanogap antenna (139/35/135 nm Au/CdS/Au). All experimental geometries are included and are labeled with the three-letter format XYZ denoting the direction of K vector, incident polarization and detection polarization, respectively.

Field distributions associated with γ and γ^* branches

Figure S4 shows simulated E_x field profiles for γ and γ^* for a 30 nm gap filled with CdS, Figures S4a and b, and a higher index ($n=3$) material, Figures S4c and d. Field distributions are consistent with our hypothesis that modes arise from the hybridization of two transverse modes on the two arms of the antenna. The lower mode, γ^* , clearly consists of anti-aligned dipoles while the higher energy γ mode shows little sign reversal. This is more evident when one removes the convolution of the conventional transverse and γ bands by increasing the optical index of the gap material to $n=3$. This shifts the gap localized modes red, Figure S4e, and offers a better view of the evolution of the modal profiles showing the appearance and red-shifting of the γ^* mode as the gap optical index is raised from 1 to 3. As described in the main text, two dielectric-side transverse modes, separated by the dielectric gap material, interact weakly when the

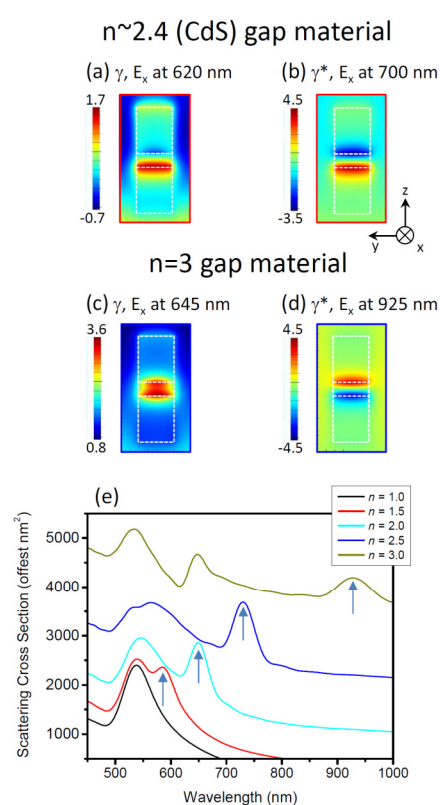


Figure S4. Field profiles associated with the proposed upper (a) and lower (b) hybridized states for a CdS gap material. Both states are localized near the gap, however, the lower energy mode exhibits a change in the sign of E_x from one gap interface to the other indicating anti-aligned dipoles. This difference becomes even clearer when the upper mode, γ , is not convoluted with the conventional transverse mode. This is done by using a higher optical index gap material. (e) Simulated spectra associated with the structures with variable gap optical index. For these simulations, light is incident along the z -direction, and polarized out-of-plane (along x). Arrows label the γ^* mode.

gap is large. As the gap shrinks, these two modes hybridize to form two states: one, a higher energy co-aligned dipole pair, Figure S4a and c, and the other, a lower energy anti-aligned dipole pair, Figure S4b and d. Plotting profiles of the largest field component, E_x , reveal the magnitude and sign of the resulting fields. The increased intensity of the mode at the bottom interface is due to the direction of incident light employed in the simulation.

Full set of EELS data

Figure S5 shows all of the EELS data sets not presented in the main manuscript. All of the nanogap antenna images were qualitatively similar, exhibiting three dominant modes which we attribute to conventional transverse (blue), gap-localized transverse (black), and longitudinal (red) modes. EELS images consistently reveal the conventional transverse mode to be localized at the antenna arm sides, the gap-localized transverse mode centered at the gap, and the longitudinal mode to have intensity at the antenna ends. The only deviation from this behavior is antenna (f), whose longitudinal mode is shifted too red to clearly measure. The data sets in Figure S5 include antennas on lacey carbon, SiN_x and Si membranes and measurements taken at 150 and 300 keV.

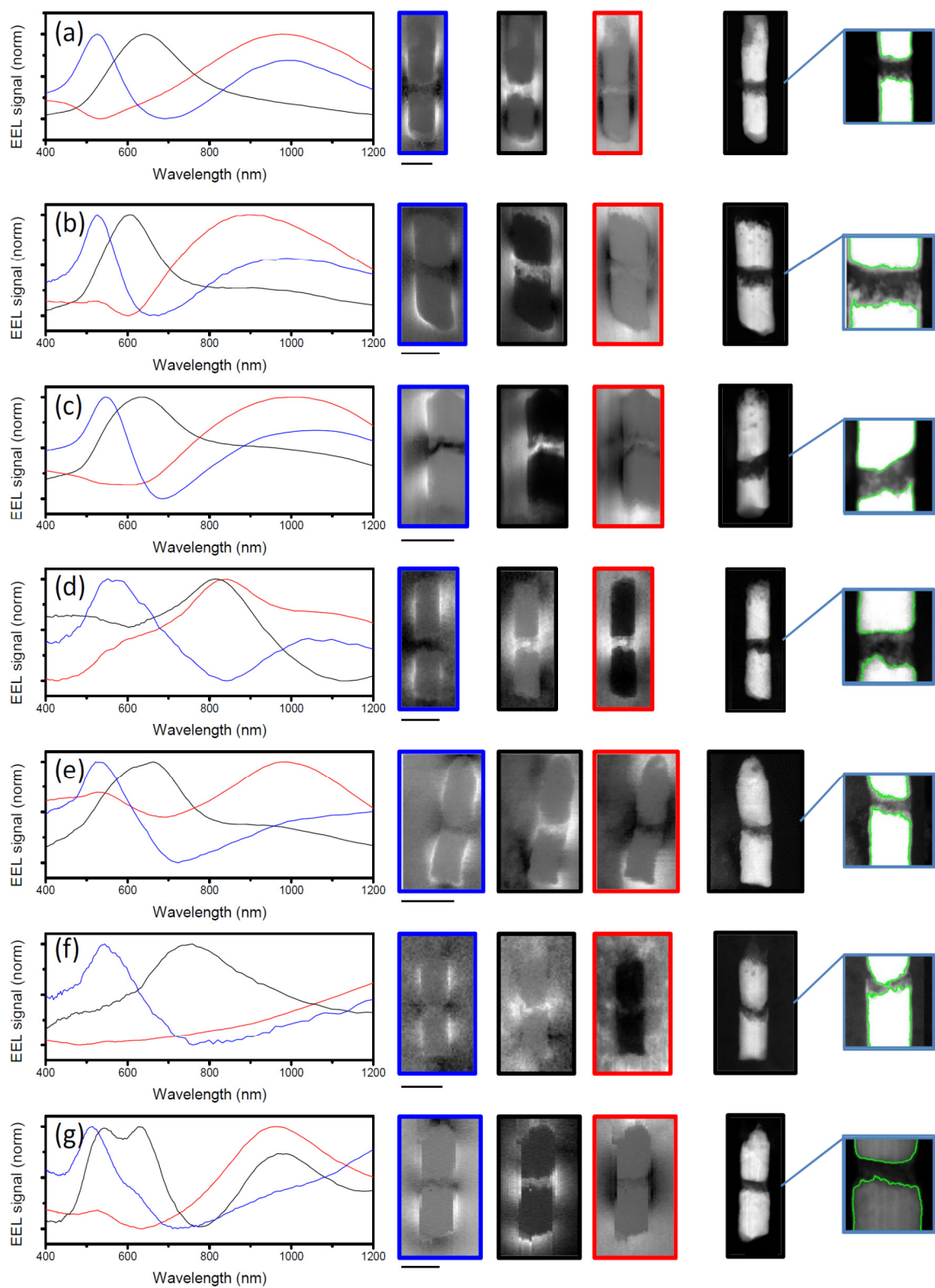


Figure S5. Additional EEL component spectra and images. Sets a-c taken on lacey carbon support at 300 kV accelerating voltage; d, e taken on SiN membranes at 300 kV; f taken on nonporous Si membrane at 300 kV; g taken on SiN membrane at 150 kV. Scale bars for each data set is 100 nm. Dark field TEM images are included as well as thresholded images of the gap structures used for measurements.

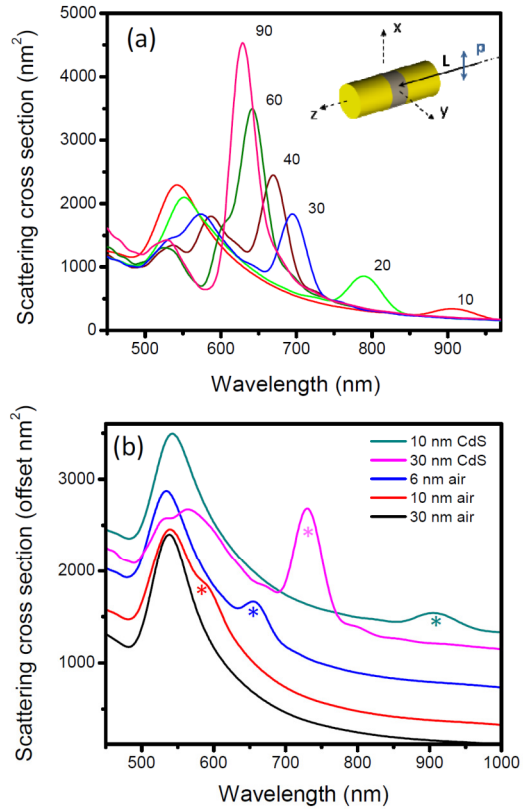


Figure S6. (a) FDTD simulated scattering spectra from a 100/x/100 nm Au/CdS/Au nanogap antenna with gap size varying from 10 to 90 nm (each curve labeled). Gap-localized transverse mode shifts red with decreasing gap size. Inset to (a) illustrates simulation geometry. (b) Comparison of gaps of varying optical index. γ and γ^* modes become visible for CdS-filled gap at larger gap sizes than for air gaps. These modes show up for air gaps but at much smaller gap sizes. γ^* modes are indicating by an *.

Gap-dependent position of gap-localized transverse mode

The spectra shown in Figure S6a were used to generate the gap-size dependent position of the gap-localized transverse mode plotted in Figure 7c of the main text. Here, we see a red shift of the gap-localized transverse peak as the gap becomes smaller, shifting from ~ 640 to ~ 910 nm for gaps shrinking from 90 to 10 nm. Figure S6b highlights the critical role of the dielectric load in the gap of these nanogap antennas in forming the gap-localized transverse mode. This mode is highly suppressed in the air-gap structure and only appears once gap sizes reach ~ 10 nm.

References

- ¹ Portela, A., Yano, T., Santschi, C., Matsui, H., Hayashi, T., Hara, M., Martin, O. J. F., Tabata, H. Spectral Tunability of Realistic Plasmonic Nanoantennas”, *Appl. Phys. Lett.* **105**, 091105 (2014).